Centre Européen de Recherche et de Formation Avancée en Calcul Scientifique

About relative and absolute logic evolutions under laws of degree 2 and 4 and in 4 dimensions at most

M. Monserrat Rincon-Camacho, Françoise Chatelin and Philippe Ricoux

Technical Report TR/PA/14/75

Publications of the Parallel Algorithms Team

http://www.cerfacs.fr/algor/publications/

ABOUT RELATIVE AND ABSOLUTE LOGIC EVOLUTIONS UNDER LAWS OF DEGREE 2 AND 4 AND IN 4 DIMENSIONS AT MOST

M. MONSERRAT RINCON-CAMACHO [(1),(2)], FRANÇOISE CHATELIN [(1),(2)], AND PHILIPPE RICOUX [(3)]

Abstract. This report is a sequel for TR/PA/14/55 and 14/68 for $l = 2$ and 4. It considers both real and complex solutions as the case may be. Then, a coupling of the real solutions provides new non real solutions. This extends the logical evolutions, relative and absolute, beyond $\mathbb{R}$ into a pencil of three numerical planes whose nature can be complex, bireal or dual.

Keywords: Logic evolution beyond $\mathbb{R}$, coupling of real roots, complex, dual, bireal numbers, triple multiplicative nature of $\mathbb{R}^2$.

1. Introduction

1.1. **An overview.** In the reports [Rincon-Camacho et al., 2014a,Rincon-Camacho et al., 2014b] we have looked at the *real* solutions of the respective equations

$$x = h(1 - |2x - 1|^l) = h\Lambda_l(x),\ h \in \mathbb{R}, \text{ and} \tag{1.1}$$

$$y = 1 - m|y|^l = G_l(m, y),\ m \in \mathbb{R}. \tag{1.2}$$

In this work, we specialise l to be 2 and 4 and consider all roots (2 and 4) provided by the Fundamental Theorem of Algebra over the *fields* $\mathbb{R}$ or $\mathbb{C}$. However this theorem does not consider the roots in $\mathbb{R}^2$ which may belong to a *ring* with zerodivisors, such as the bireals in ${}^2\mathbb{R} = \mathbb{R} \oplus \mathbb{R}u$, $u^2 = 1$, $u \neq \pm 1$, and the duals in $\mathbb{D} = \mathbb{R} \oplus \mathbb{R}n$, $n^2 = 0$, $n \neq 0$. See [Rincon-Camacho and Latre, 2013, Chatelin, 2016, chapter 2] for more.

By allowing the coupling of the real roots, we extend the *real* logic evolutions defined by the laws $h\Lambda_l$ and G_l, which were presented earlier. When real and complex roots coexist, the logic evolution becomes *trine*: it takes values in the 4D-space $\mathbb{R}^4$ spanned by $\{1, i, n, u\}$ where the squares of the non real vectors are respectively -1, 0, 1. The 2D-solutions of (1.1) or (1.2) belong to the pencil of *three* orthogonal planes $\mathbb{C} \cup \mathbb{D} \cup {}^2\mathbb{R}$ for $l = 4$. The pencil reduces to *two* planes for (1.1) when $l = 2$.

1.2. **Quantitative representation in $\mathbb{R}^2$ and $\mathbb{R}^3$.** The newly introduced 2D-solutions are denoted $\hat{x}(h)$ and $\hat{y}(m)$ and are written generically as $\alpha + \omega\beta$ where $\omega \in \{i, n, u\}$. If the *triple* nature of ω is not taken into account, one may represent the maps $\hat{x}$ and $\hat{y}$ in $\mathbb{R}^3$, as well as the two component maps α and β in $\mathbb{R}^2$.

2. Quadratic evolutions, $l = 2$

2.1. $x = h\Lambda_2(x)$, $h \in \mathbb{R}$.

(1) CEREMATH, Université Toulouse 1, 21, Allée de Brienne, 31000 Toulouse, France. (rincon@cerfacs.fr).
(1),(2) CERFACS, 42, avenue Gaspard Coriolis, 31057 Toulouse, France. (chatelin@cerfacs.fr).
(3) TOTAL SA Direction Scientifique, 24, cours Michelet LA DEFENSE 10, 92069 Paris La Defense CEDEX, France. (philippe.ricoux@total.com).

The equation

$$x = 4hx(1-x) \;\Leftrightarrow\; x\left(x - \frac{1}{4h}\right) = 0, \;\; h \neq 0 \tag{2.1}$$

has the two real roots $x_1 = 0$ and $x_2 = 1 - \frac{1}{4h}$, $h \neq 0$ which are distinct for $h \neq \frac{1}{4}$.

The coupling yields the following new roots outside $\mathbb{R}$:

- $h \notin \{0, \frac{1}{4}\}$, $\hat{x}(h) = \frac{1}{2}(1 - \frac{1}{4h})(1 \pm u) = (1 - \frac{1}{4h})e_{\pm}$ in ${}^2\mathbb{R}$, that is $\alpha = \pm\beta = \frac{1}{2} - \frac{1}{8h}$,
- $h = \frac{1}{4}$, $\hat{x}(\frac{1}{4}) \in n\mathbb{R}^*$ in $\mathbb{D}$, that is $\alpha = 0$, β arbitrary.

The new solutions for (2.1), $h \neq 0$, are zerodivisors, being proportional to an idempotent e_+ or e_-, or to a nilpotent n. The logic is dual in ${}^2\mathbb{R} \cup \mathbb{D}$.

2.2. $\boldsymbol{y = G_2(m, y)}$, $\boldsymbol{m \in \mathbb{R}}$.

The equation

$$y = 1 - my^2 \;\Leftrightarrow\; y^2 + \frac{1}{m}y - \frac{1}{m} = 0, \;\; m \neq 0 \tag{2.2}$$

has 2 roots whose nature depends on $\Delta = 1 + 4m$. There are three cases, leading to a trine logic:

- $m < -\frac{1}{4}$, $\hat{y}_{\pm}(m) = \frac{1}{2m}(1 \pm i\sqrt{-\Delta}) \in \mathbb{C}$,
- $m = -\frac{1}{4}$, $\hat{y}(\frac{1}{4}) \in 2 + n\mathbb{R}$ in $\mathbb{D}$,
- $m > -\frac{1}{4}$, $\hat{y}_{\pm}(m) = \frac{1}{2m}(1 \pm u\sqrt{\Delta}) \in {}^2\mathbb{R} \setminus \mathbb{R}$.

For $m \neq \frac{1}{4}$, $\alpha = \frac{1}{2m}$, $\beta = \pm\frac{1}{2m}\sqrt{|\Delta|}$, and for $m = \frac{1}{4}$, $\alpha = 2$, β arbitrary.

Lemma 2.1. *For $m \neq 0$, $\mu(\hat{y}) = -\frac{1}{m}$ and $\mu(\hat{y} - 1) = 1$.*

Proof. Use $\mu(\hat{y}) = \hat{y}\hat{y}^*$. For example, in ${}^2\mathbb{R}$ $\hat{y} - 1 = \frac{1}{2m}(1 - 2m + u\sqrt{\Delta})$ and $\hat{y}^* - 1 = \frac{1}{2m}(1 - 2m - u\sqrt{\Delta})$, then $\mu(\hat{y} - 1) = \frac{1}{4m^2}[(1-2m)^2 - 1 - 4m] = 1$. □

2.3. **Quantitative representations.**

See Figure 1

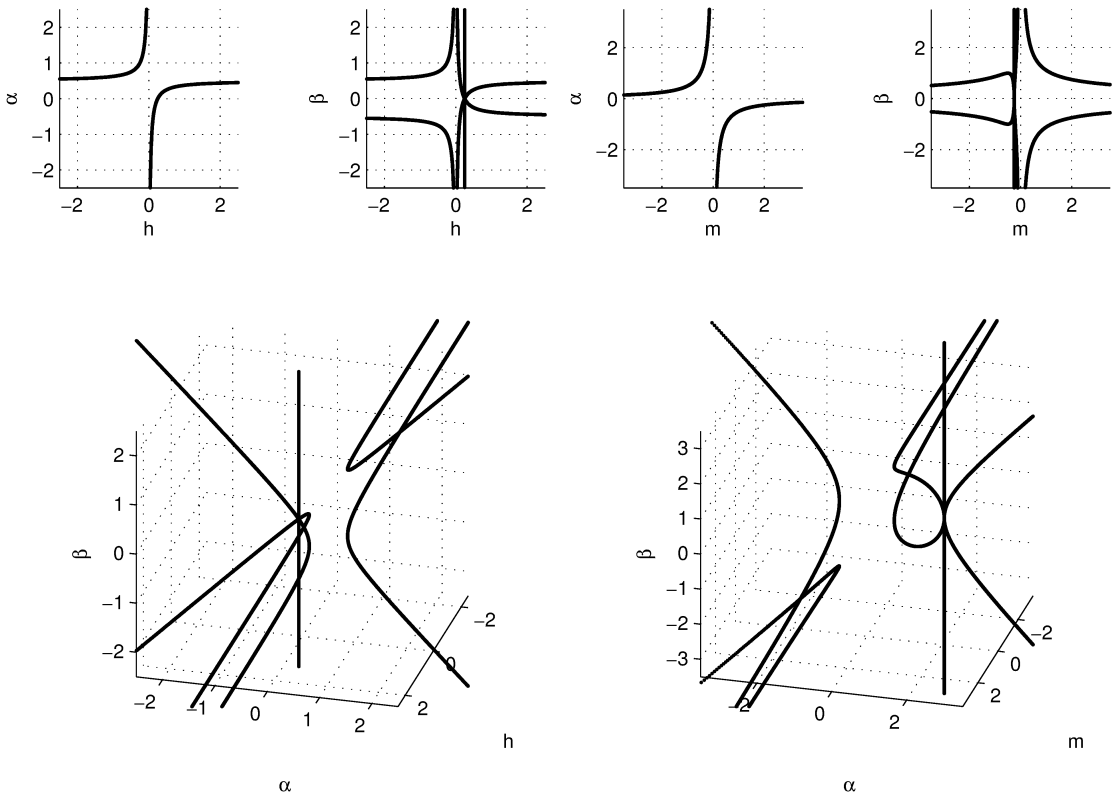

(a) $h \mapsto (\alpha, \beta)$ (b) $m \mapsto (\alpha, \beta)$

FIGURE 1. $l = 2$

3. Quartic evolutions, $l = 4$

3.1. $\boldsymbol{x = h\Lambda_4(x)}$, $\boldsymbol{h \in \mathbb{R}}$.

The roots of equation

$$x = h(1-(2x-1)^4) \;\Leftrightarrow\; x\left(x^3 - 2x^2 + \frac{3}{2}x + \frac{1}{16h} - \frac{1}{2}\right) = 0,\ h \neq 0 \tag{3.1}$$

have been studied in Section 2.4 of [Rincon-Camacho et al., 2014a], see (2.3) therein. Beside $x = 0$ (simple for $h \neq \frac{1}{8}$ and double for $h = \frac{1}{8}$) there exists another real root $x_1(h) = -2r(h)\sinh\frac{\varphi}{3} + \frac{2}{3}$ where $\varphi = \varphi(h) \geq 0$, $h \neq 0$, $r(h) = (\operatorname{sgn} q)\frac{1}{3\sqrt{2}}$. The associated pair of complex conjugate roots is provided by (A.12): $\hat{x}_\pm(h) = \frac{2}{3} + r(h)(\sinh\frac{\varphi}{3} \pm i\sqrt{3}\cosh\frac{\varphi}{3})$ with $\varphi \geq 0$, $h \neq 0$.

The coupling of the two real roots $x = 0$ and $x_1(h)$ yields new unreal roots:

- $h \notin \{0, \frac{1}{8}\}$, $\quad \hat{x}_\pm(h) = \frac{1}{2}(-r(h)\sinh\frac{\varphi}{3} + \frac{1}{3})(1 \pm u) = (-2r(h)\sinh\frac{\varphi}{3} + \frac{2}{3})e_\pm \in {}^2\mathbb{R} \setminus \mathbb{R}$,
- $h = \frac{1}{8}$, $\quad \hat{x}(\frac{1}{8}) \in n\mathbb{R}^*$ in $\mathbb{D}$.

As for the quadratic evolution, the new solutions are zerodivisors.

Lemma 3.1. *For $h \neq 0$, the complex conjugate pair $\hat{x}_\pm = \alpha \pm i\beta$ describes the hyperbola*

$$\beta^2 - 3\left(\alpha - \frac{2}{3}\right)^2 = \frac{1}{6}. \tag{3.2}$$

Proof. $\sinh \frac{\varphi}{3} = \frac{1}{r}(\alpha - \frac{2}{3}) = (\mathrm{sgn}\, q)3\sqrt{2}(\alpha - \frac{2}{3})$, $\cosh \frac{\varphi}{3} = \frac{1}{r\sqrt{3}}\beta = (\mathrm{sgn})\sqrt{6}\beta$ for $q \neq 0 \Leftrightarrow \varphi \neq 0$; $\varphi = 0$ for $h = h'$. Then $6\beta^2 - 18(\alpha - \frac{2}{3})^2 = 1$ establishes (3.2).

The centre of the hyperbola is $(\frac{2}{3}, 0)$ and the slopes of the asymptotes are $\pm\sqrt{3}$. The tips of the branches occur for $h = h' = 0.675$ with values $(\frac{2}{3}, \pm\frac{1}{\sqrt{6}})$. □

3.2. $y = G_4(m, y)$, $m \in \mathbb{R}$.

The real roots of the equation

$$y = 1 - my^4 \;\Leftrightarrow\; y^4 + \frac{1}{m}y - \frac{1}{m} = 0,\; m \neq 0 \tag{3.3}$$

have been studied in Section 2.4 of [Rincon-Camacho et al., 2014b]. For $l = 4$, $m_0 = -\frac{3^3}{4^4} \approx -0.1055$ and $y(m_0) = \frac{4}{3}$. Using z as the unique positive solution of the auxiliary equation (2.2) $z^3 + \frac{1}{m}z - \frac{1}{8m^2} = 0$, the roots of (3.3) satisfy the pair of quadratic equations

$$y^2 \pm \sqrt{2z}\, y + z \mp \frac{1}{2m\sqrt{2z}} = 0 \tag{$Q_\pm$}$$

with discriminant $\Delta_\pm = -2z \pm \frac{1}{m}\sqrt{\frac{2}{z}}$.

We recall the table

m		m_0		0	
Δ_-	$-$	0	$+$	|	$-$
Δ_+	$-$		$-$	|	$+$
nature of roots	(1)	(2)	(3)	|	(3)

where (1) refers to 2 pairs of complex conjugate (c.c.) numbers,
(2) " 1 double root $\frac{4}{3}$ and 1 c.c. pair,
(3) " 2 real numbers $s \neq s'$ and 1 c.c. pair.

The real roots occur for $m \geq m_0$. Their coupling yields either $\hat{y}(m_0) \in \frac{4}{3} + n\mathbb{R}$ in $\mathbb{D}$ or for $m > m_0$ the 4 numbers s, s', $se_+ \pm s'e_- = \frac{s+s'}{2} \pm \frac{s-s'}{2}$ in ${}^2\mathbb{R}$.

Setting again $\hat{y}_\pm = (\alpha, \pm\beta)$, it follows that $\alpha = \mp\sqrt{\frac{z}{2}}$ and $|\beta| = \frac{1}{2}|\Delta_\pm(m)|^{1/2}$. Let $\boldsymbol{\tau}$ denote any trigonometric function cos, cosh, sinh then with $\varphi(m)$ defined by $\boldsymbol{\tau}(\varphi(m)) = \frac{3\sqrt{3}}{16\sqrt{|m|}}$, $z = \frac{2}{\sqrt{|m|}}\boldsymbol{\tau}(\frac{\varphi(m)}{3})$. Hence there is no *algebraic* expression for z in terms of an arbitrary m. However if $m = m_0$, $D(m_0) = 0$, $\cos\varphi = \cosh\varphi = 1 \Leftrightarrow \varphi = 0$, $z(m_0) = -2r(m_0) = \frac{2}{\sqrt{-3m_0}} = \frac{2^5}{3^2} = \frac{32}{9}$, $\sqrt{2z} = \frac{8}{3}$. The evolutions $m \mapsto (\alpha, \beta)$ will be experimentally studied in Section 4.3.

3.3. **Quantitative representations.**

See Figure 2

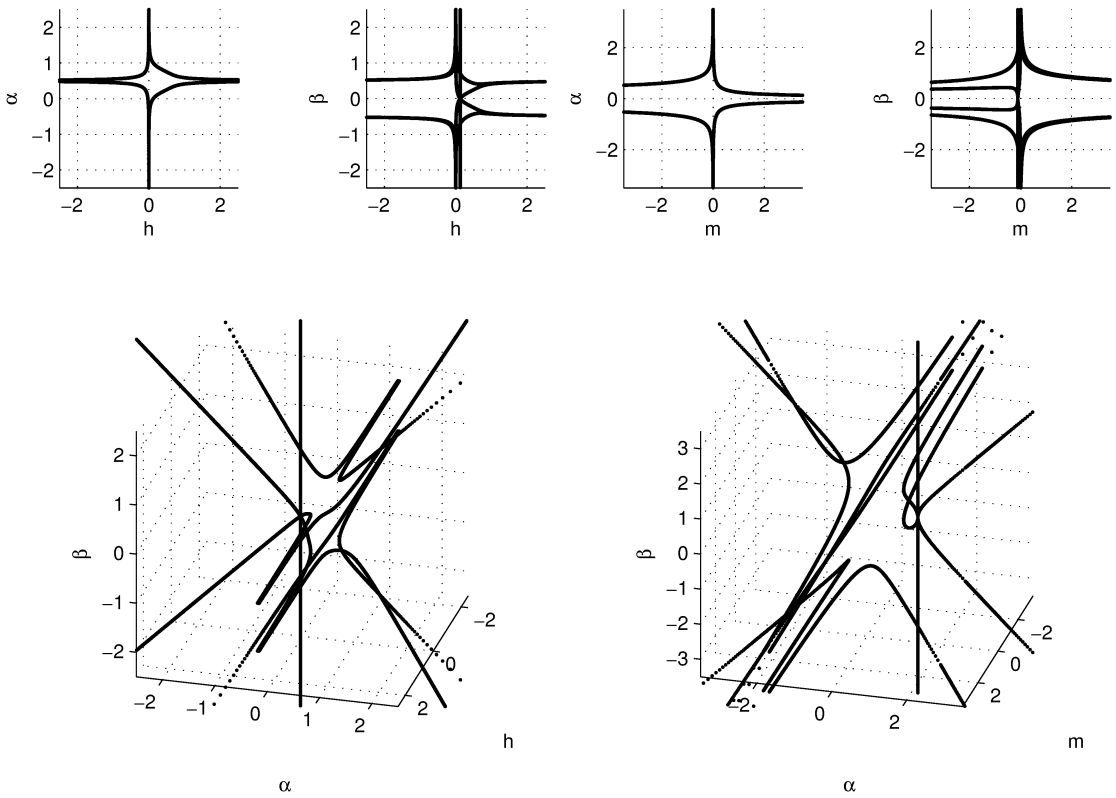

(a) $h \mapsto (\alpha, \beta)$ (b) $m \mapsto (\alpha, \beta)$

FIGURE 2. $l = 4$

4. Qualitative evolutions in planes

As the parameter h (resp. m) varies in $\mathbb{R}$, there are two exceptional values: 0 where x (resp. y) is not defined and $h_0 = \frac{1}{2l}$ (resp. $m_0 = -\frac{(l-1)^{l-1}}{l^l}$) where $x = 0$ (resp. $y = \frac{l}{l-1}$) is a double root. Both values signal a singularity.

These 2 values delineate 3 intervals for the variation of the parameter to which are assigned the three colours red-yellow-blue of decreasing hue as the parameter increases. To the transition value $h_0 > 0$ (resp. $m_0 < 0$) is attributed the colour green (resp. orange).

The next two sections represent the parametric evolutions of the real and 2D-solutions in the real plane of triple nature by means of the corresponding colour chart for the parameter variation.

4.1. $x = h\Lambda_l(x)$, $l = 2$ and 4, $x(h_0) = 0$.

Colour chart for $h \in \mathbb{R}$

Figure 3 (resp. 4) corresponds to $l = 2$ (resp. 4).

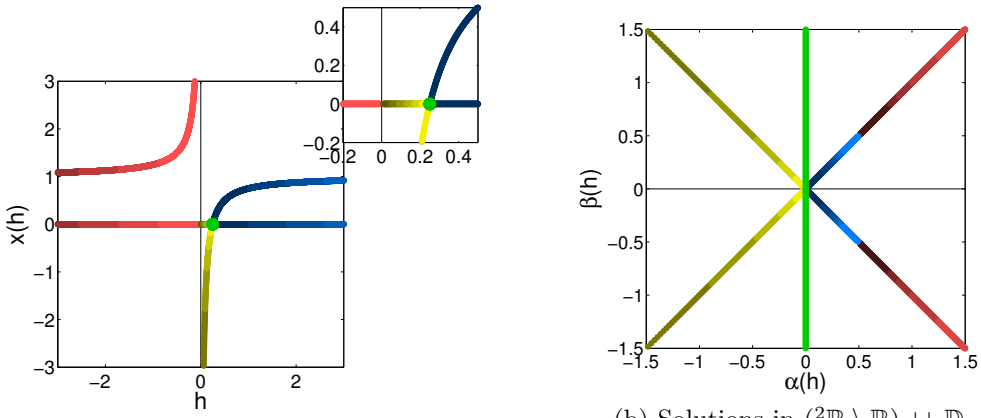

(a) Solutions in $\mathbb{R}$ (b) Solutions in $({}^2\mathbb{R} \setminus \mathbb{R}) \cup \mathbb{D}$

FIGURE 3. $l = 2$: Solutions to $x = h\Lambda_2(x)$ in 1 and 2 dimensions

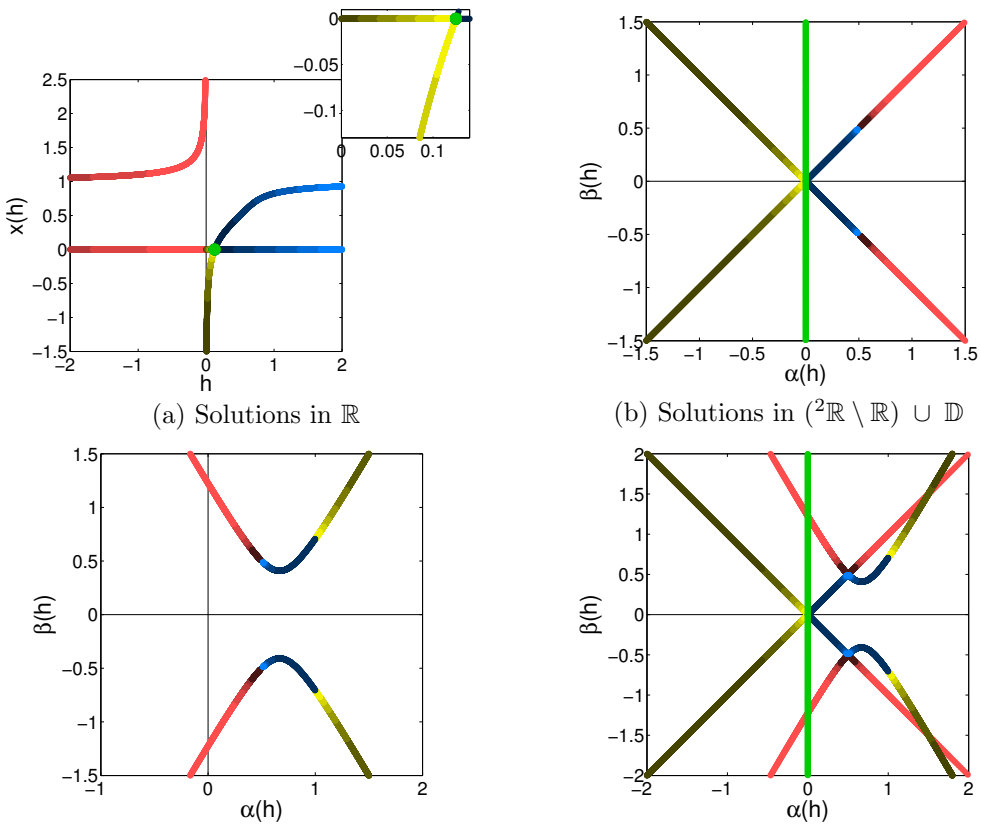

(a) Solutions in $\mathbb{R}$ (b) Solutions in $({}^2\mathbb{R} \setminus \mathbb{R}) \cup \mathbb{D}$

(c) Solutions in $\mathbb{C}$ (d) Solutions in $({}^2\mathbb{R} \setminus \mathbb{R}) \cup \mathbb{D} \cup \mathbb{C}$

FIGURE 4. $l = 4$: Solutions to $x = h\Lambda_4(x)$ in 1 and 2 dimensions

We observe that the evolution in $({}^2\mathbb{R}\setminus\mathbb{R})\cup\mathbb{D}$ is unchanged from $l=2$ to 4. The only change is the *complex* hyperbola for $l=4$. The discontinuity in h from $+\infty$ to $-\infty$ (blue - red), which shows for $\alpha=|\beta|=\frac{1}{2}$, corresponds to $\hat{x}_\pm = e_\pm$.

4.2. $y = G_l(m,y)$, $l=2$ and 4, $y(m_0)=\frac{l}{l-1}$.

Color chart for $m\in\mathbb{R}$

Figure 5 (resp. 6) corresponds to $l=2$ (resp. 4)

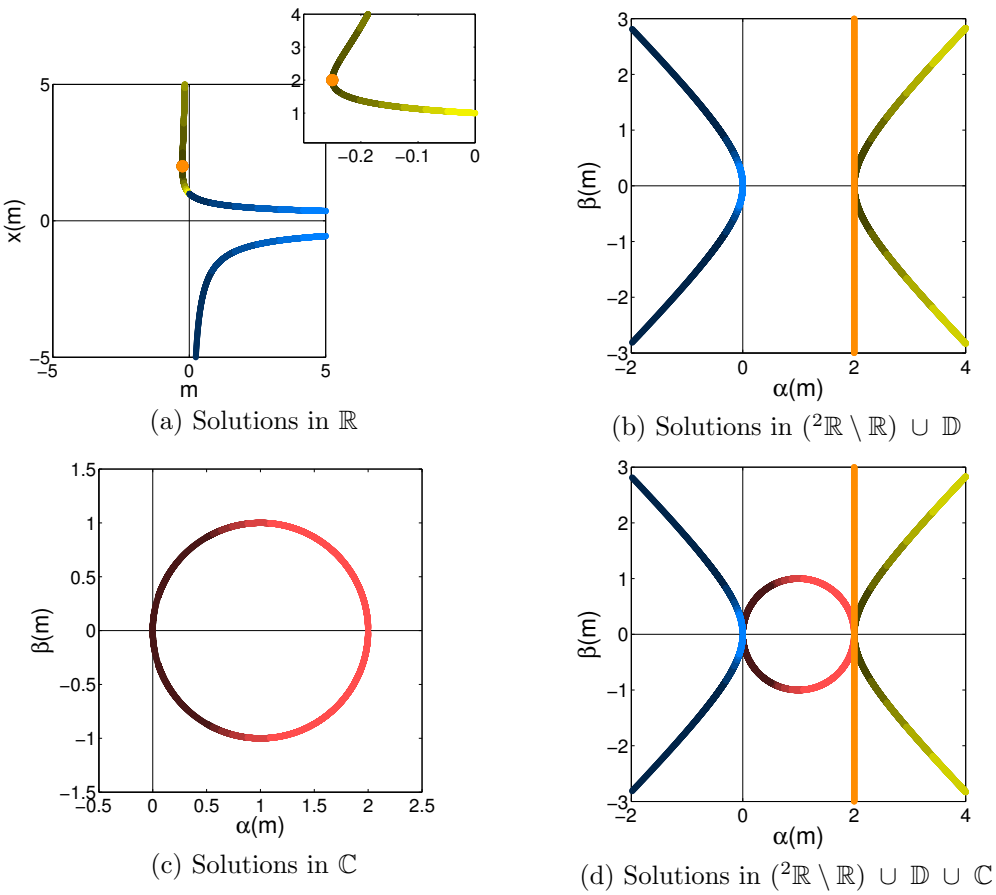

(a) Solutions in $\mathbb{R}$

(b) Solutions in $({}^2\mathbb{R}\setminus\mathbb{R})\cup\mathbb{D}$

(c) Solutions in $\mathbb{C}$

(d) Solutions in $({}^2\mathbb{R}\setminus\mathbb{R})\cup\mathbb{D}\cup\mathbb{C}$

FIGURE 5. $l=2$: Solutions to $y=G_2(m,y)$ in 1 and 2 dimensions, $m_0=-\frac{1}{4}$, $y(-\frac{1}{4})=2$

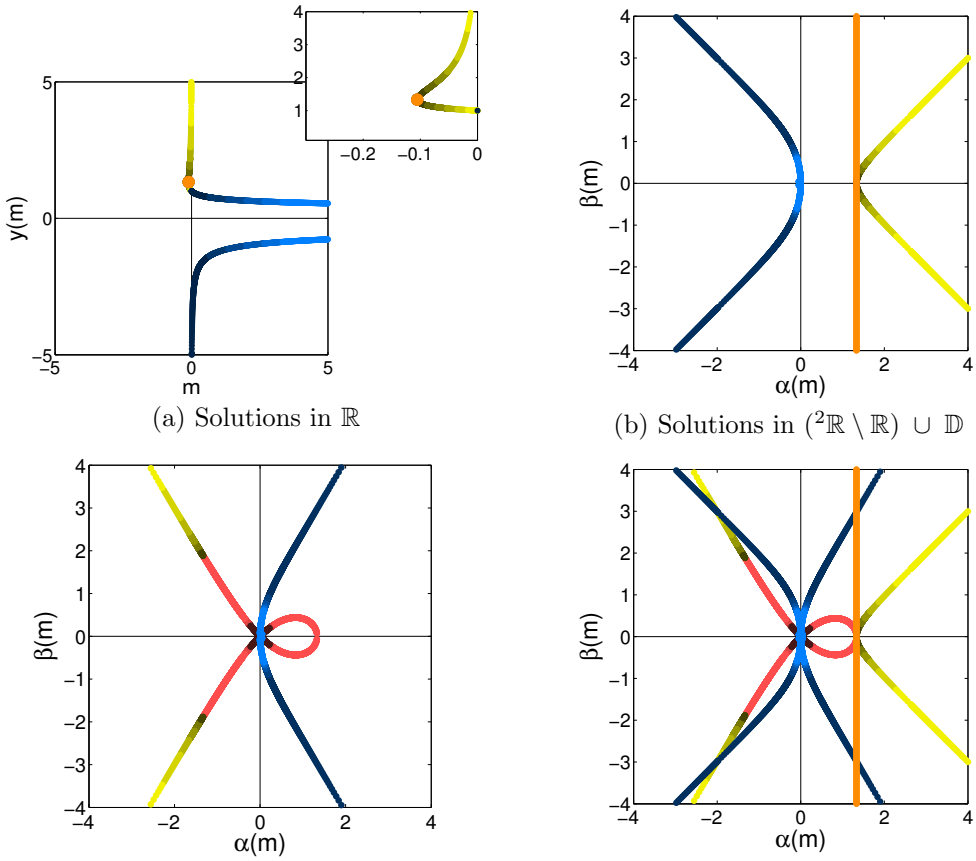

(a) Solutions in $\mathbb{R}$

(b) Solutions in $({}^2\mathbb{R} \setminus \mathbb{R}) \cup \mathbb{D}$

(c) Solutions in $\mathbb{C}$

(d) Solutions in $({}^2\mathbb{R} \setminus \mathbb{R}) \cup \mathbb{D} \cup \mathbb{C}$

FIGURE 6. $l = 4$: Solutions to $y = G_4(m, y)$ in 1 and 2 dimensions, $m_0 = -\frac{3^3}{4^4}$, $y(m_0) = \frac{4}{3}$

When $l = 2$, the behaviour is such that $\mu(\hat{y} - 1) = 1$. With $\hat{y} = (\alpha, \beta)$ this leads to the hyperbola $(\alpha - 1)^2 - \beta^2 = 1$ for $m > m_0$, the dual line $\alpha = 2$ for $m_0 = -\frac{1}{4}$ and the circle $(\alpha - 1)^2 + \beta^2 = 1$ for $m < m_0$.

The red partial curve $m < m_0$ correspond to $|\alpha| < \frac{1}{2}\sqrt{2z(m_0)} = \frac{4}{3}$, $|\beta| < |\Delta_+(m_0)|^{1/2} = \frac{4}{3}\sqrt{2} \approx 1.8856$. We study experimentally in more detail the case $l = 4$ in the next section.

4.3. $y = G_4(m, y)$.

Figure 7 displays the asymptotes $\beta = \pm(\alpha - 1)$ for the bireal behaviour, corresponding to $m \to 0$.

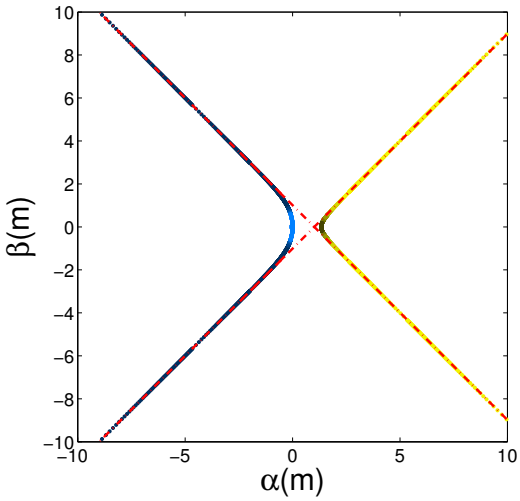

FIGURE 7. The asymptotes $\beta = \pm(\alpha - 1)$ as $m \to 0$ in ${}^2\mathbb{R}$

A zoom near $m = \infty$ in the bireal plane is displayed by Figure 8. The left blue curve points at 0 to a computational artefact discussed in Section 6.4.

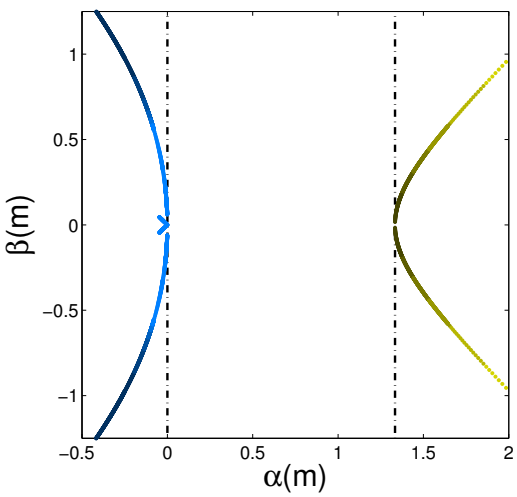

FIGURE 8. $\lim_{m\to\infty} \hat{y}(m) = (0,0)$ and $\lim_{m\to m_0} y(m) = (\frac{4}{3}, 0)$ in ${}^2\mathbb{R}$

We turn to the complex plane. See Figure 9 for $m \to 0$ and Figure 10 for a zoom around 0 when $|m| \to \infty$.

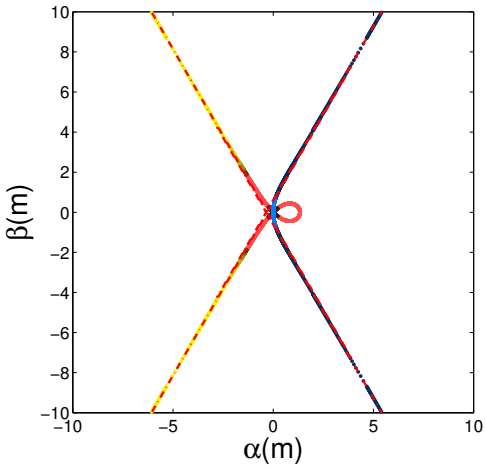

FIGURE 9. The asymptotes $\beta = \pm(\sqrt{3}\alpha + \frac{1}{\sqrt{3}})$ as $m \to 0$ in $\mathbb{C}$

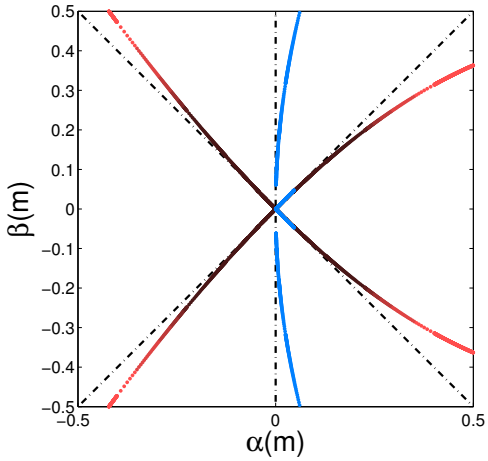

FIGURE 10. The slopes are ± 1, ∞ at $(0,0)$ in $\mathbb{C}$

Figure 11 provides two zooms on the loop obtained in $\mathbb{C}$ for $m < m_0$. Two computed inscribed circles are displayed in black. In Figure 11 (a) the circle passes through $(\frac{4}{3}, 0)$, and in Figure 11 (b) the circle is tangent to the loop horizontally.

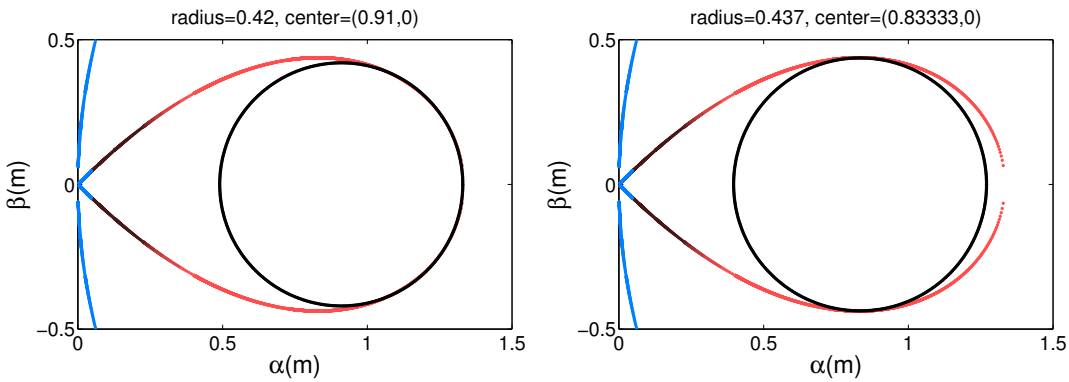

(a) (b)

FIGURE 11. The complex loop for $m < m_0$

A careful inspection of Figure 11 suggests a jump from $m = +\infty$ to $m = -\infty$ near 0, a phenomenon already encountered on Figure 10 and clearly visible on Figure 8. We propose a partial explanation in Section 6.4 below.

5. When the parameter vanishes

5.1. **Over $^2\mathbb{R}$.** When h or m tends to 0, the pair of real solutions undergoes a discontinuity:

- for Λ_l, $(0, x(h))$ tends to $(0, +\infty)$ as $h \to 0^-$ and to $(0, -\infty)$ as $h \to 0^+$,

• for G_l, $(y_1(h), y_2(h))$ tends to $(1, +\infty)$ as $m \to 0^-$ and to $(1, -\infty)$ as $m \to 0^+$.
This shows in the *bireal* plane on the lines $\beta = \pm\alpha$ for Λ and on the asymptotes $\beta = \pm(\alpha - 1)$ for G which meet respectively at $(0, 0)$ and $(1, 0)$.

5.2. **Over $\mathbb{C}$.** The picture gets more contrasted between $l = 2$ and 4 in the *complex* plane. On the one hand, there is no complex roots for Λ_2 and, when they exist for G_2, they do not escape to ∞ but rather describe a unit circle centered at $(1, 0)$. On the other hand, the complex roots describe a hyperbola for Λ_4 centered at $(\frac{2}{3}, 0)$ and 2 distinct curves for G_4. The yellow-red curve is better considered as consisting of two parts according to the 2 colours.

On the red curve corresponding to $m < m_0$, $|\alpha| \leq \frac{4}{3}$, no complex roots can escape to ∞. This red curve is the analogue for G_4 of the red circle for G_2.

By contrast, on the yellow curve ($m_0 < m < 0$), complex pairs do escape to ∞ in modulus as $m \to 0^-$. The same is true on the blue curve ($m > 0$) as $m \to 0^+$. The asymptotes have slopes $\pm\sqrt{3}$, as for Λ_4, but they meet at $(-\frac{1}{3}, 0) = (\frac{2}{3}, 0) - (1, 0)$.

6. When the parameters escape to $\pm\infty$

6.1. **Over $\mathbb{R}$.** As $|h| \to \infty$, the pair of real roots $(0, x(h))$ for Λ converges to $(0, 1)$ where $0 \neq 1$. By contrast, for G, the real roots $y_1(m)$ and $y_2(m)$ converge each to 0 which becomes double ($l = 2$) or quadruple ($l = 4$) for $|m| \to \infty$.

6.2. **Over $^2\mathbb{R}$.** The coupling of 0 and 1 for Λ yields the idempotent pair $\frac{1}{2}(1 \pm u) = e_\pm$. It shows on Figures 3 (b) and 4 (b) by a jump for h from blue ($h = +\infty$) to red ($h = -\infty$) at $\alpha = |\beta| = \frac{1}{2}$ ($\hat{x} = e_\pm$). As for G, since 0 appears multiple at ∞, the coupling yields the dual axis $n\mathbb{R}$ for $m = +\infty$, represented as the light blue dual axis on Figure 12.

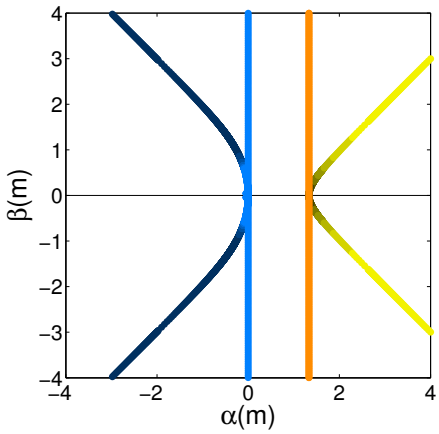

Figure 12. $m \in \mathbb{R} \cup \{+\infty\}$

6.3. **Over $\mathbb{C}$.** There is nothing more to add for Λ, hence we turn to G_l. If m is allowed to vary in the extended line $\bar{\mathbb{R}} = \mathbb{R} \cup \{\pm\infty\}$, then the dual axis is obtained for $m = -\infty$ if $l = 2$ and for $m = \pm\infty$ if $l = 4$. It is represented in the later case as a violet (=red+blue) line on Figure 13.

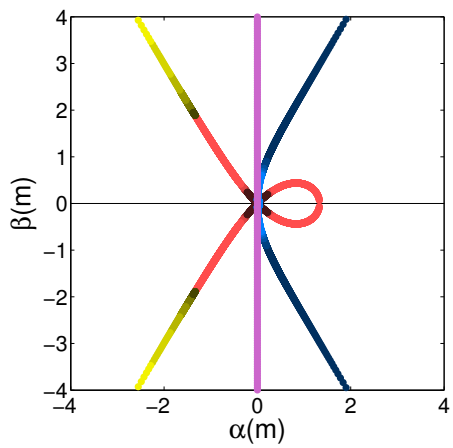

FIGURE 13. $m \in \mathbb{R} \cup \{+\infty\}$

6.4. **About numerical artefacts for G_4 around 0 ($|m|$ large enough).** We can explain the artefact on Figure 8 as a result of the coupling for $m > 0$ very large of the two real variables $y_1(m) > 0$ and $y_2(m) < 0$. They both tend to 0 as $m \to \infty$ with *different* speeds: y_1 tends to 0^+ faster than y_2 to 0^-. Therefore, for m large enough, computation sees $y_1 = 0$ and $0 \neq y_2 < 0$. The coupling of 0 and y_1 yields the bireal numbers $y_1(\frac{1\pm u}{2}) = y_1 e_\pm$ for $y_1 < 0$ small enough.

The explanation of the superposition of a blue line ($m \to \infty$) and red near the origin on the top of the red loop ($m \to -\infty$) requires to consider the coupling of two numbers of a different nature, one real and one complex, both converging to 0 as $m \to \infty$.

Such a coupling ($\mathbb{R}$ and $\mathbb{C}$) as well as $\mathbb{C}$ with $\mathbb{C}$ is beyond the limited scope of this report. We only mention that this can be done in the framework of the ring of bicomplexes ${}^2\mathbb{C} = \mathbb{C} \oplus \mathbb{C}u$ spanned by the 4 vectors 1, i, u, iu where u is a unipotent number ($u^2 = 1$) and i, iu are complex numbers (square $= -1$), all numbers with 4 real dimensions [Chatelin, 2016, Rincon-Camacho and Latre, 2013].

7. CONCLUSION

The quantitative representations of real roots couplings given by Figures 14 and 15 are displayed below in the three colours red-yellow-blue, where the readability of yellow curves is enhanced by means of a gray shade.

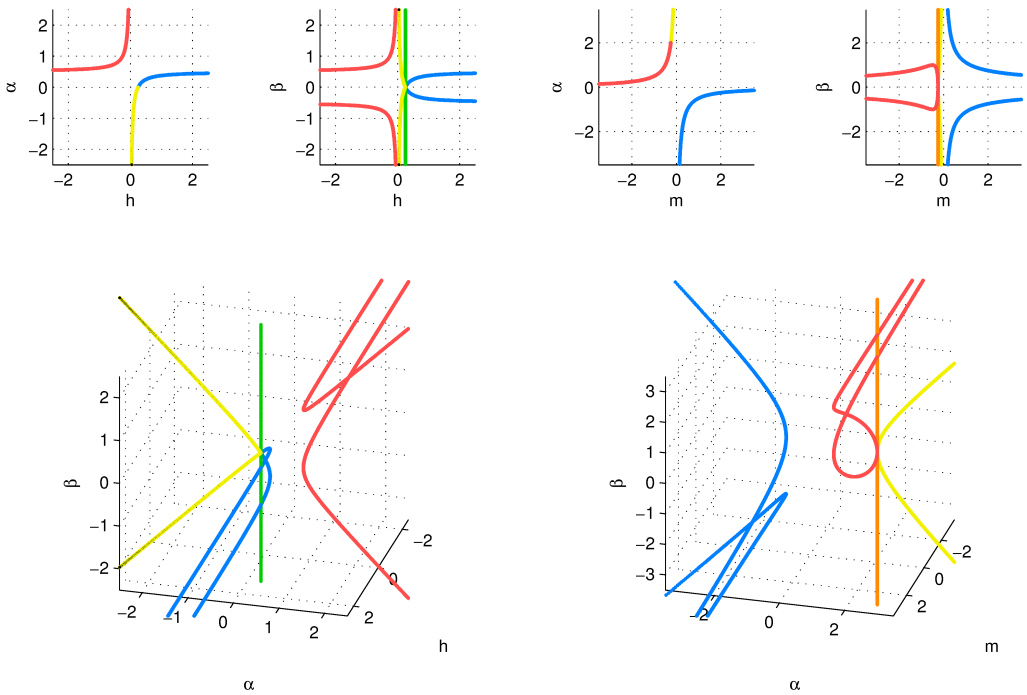

(a) $h \mapsto (\alpha, \beta)$
green line at $(\frac{1}{4}, 0)$

(b) $m \mapsto (\alpha, \beta)$
orange line at $(-\frac{1}{4}, 2)$

FIGURE 14. $l = 2$

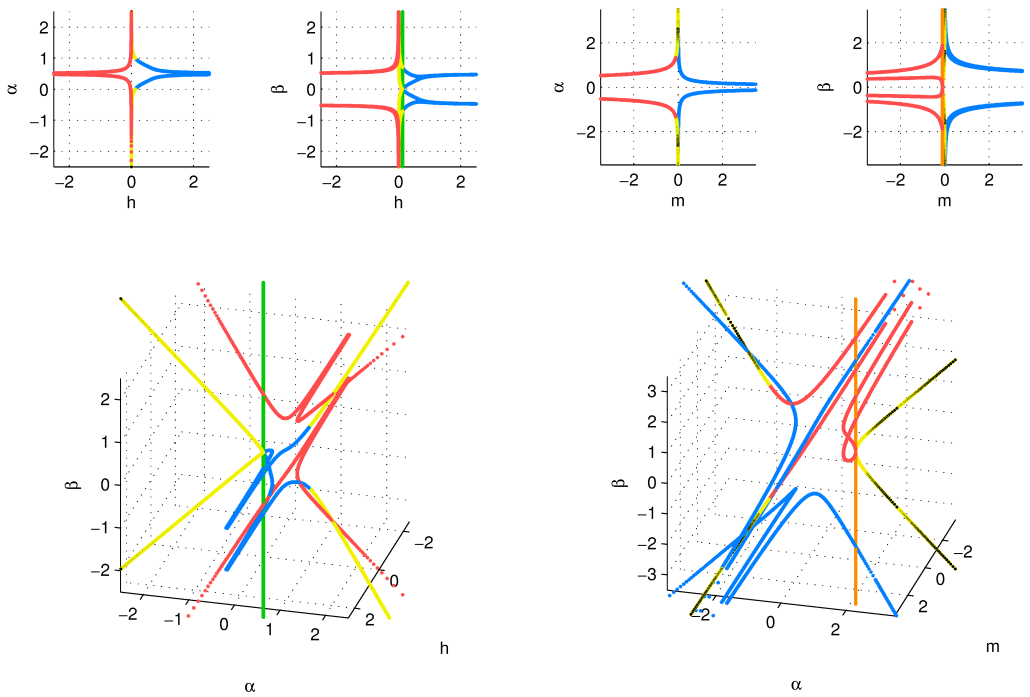

(a) $h \mapsto (\alpha, \beta)$
green line at $(\frac{1}{8}, 0)$

(b) $m \mapsto (\alpha, \beta)$
orange line at $(-\frac{3^3}{4^4}, \frac{4}{3})$

FIGURE 15. $l = 4$

The philosophically inclined reader is referred to the report [Chatelin and Rincon-Camacho, 2014] which presents some epistemological views on the comparative evolutions of the numbers 0 and 1 as numbers with 1 and 2 dimensions under the absolute and relative laws 1.2 and 1.1 respectively.

Acknowledgement M. M. Rincon-Camacho is grateful for the financial support from the Scientific Direction TOTAL through the contract DS-2755-B with Cerfacs (Qualitative Computing group).

REFERENCES

[Chatelin, 2016] Chatelin, F. (2016). *Numbers in Mind: The transformative dynamics of Numerics (in preparation)*. World Scientific and Imperial College Press, London.

[Chatelin and Rincon-Camacho, 2014] Chatelin, F. and Rincon-Camacho, M. M. (2014). Organic Information Theory: living and feeling beyond the boolean world. Submitted to *Frontiers in Neuroscience*.

[Rincon-Camacho et al., 2014a] Rincon-Camacho, M. M., Chatelin, F., and Ricoux, P. (2014a). About a family of logistic equation based on a relative distance to $\frac{1}{2}$ raised to a positive power. Technical report, CERFACS TR/PA/14/55.

[Rincon-Camacho et al., 2014b] Rincon-Camacho, M. M., Chatelin, F., and Ricoux, P. (2014b). Beyond Boolean logic. A family of logistic equations as a model for numerical evolution of the fixed points 0 and 1 for multiplication. Technical report, CERFACS TR/PA/14/68.

[Rincon-Camacho and Latre, 2013] Rincon-Camacho, M. M. and Latre, J.-B. (2013). Project description: Algebraic structures for information processing associated with Dickson algebras. Technical report, CERFACS TR/PA/13/106.